Particle-Filtering-Based Prognosis Framework for Energy Storage Devices With a Statistical Characterization of State-of-Health Regeneration Phenomena

Benjamín E. Olivares, Matías A. Cerda Muñoz,
Marcos E. Orchard, *Member, IEEE*, and Jorge F. Silva, *Member, IEEE*

***Abstract*—This paper presents the implementation of a particle-filtering-based prognostic framework that allows estimating the state of health (SOH) and predicting the remaining useful life (RUL) of energy storage devices, and more specifically lithium-ion batteries, while simultaneously detecting and isolating the effect of self-recharge phenomena within the life-cycle model. The proposed scheme and the statistical characterization of capacity regeneration phenomena are validated through experimental data from an accelerated battery degradation test and a set of *ad hoc* performance measures to quantify the precision and accuracy of the RUL estimates. In addition, a simplified degradation model is presented to analyze and compare the performance of the proposed approach in the case where the optimal solution (in the mean-square-error sense) can be found analytically.**

***Index Terms*—Capacity regeneration, energy storage devices (ESDs), particle filters (PFs), SOH prognosis, state-of-health (SOH) monitoring.**

I. Introduction

ENERGY STORAGE devices (ESDs), and particularly lithium-ion batteries, have played a significant role in the development of novel and more efficient communication, transportation, and mobile systems. They do not only represent the means to manage energy resources (securing the availability of electric supply for time-varying power demand even when the system is isolated), but they are also an important constraint in terms of the maximum autonomy that any of those systems may attain.

In recent years, the criticality of this role has increased as a result of the exponential growth of the industry of cell phones, laptop computers, autonomous ground and unmanned aerial vehicles, and hybrid and electric vehicles, among other electronic systems. Regardless of the main purpose for which these technologies are being developed, it is a fact that end users expect at least three main features from the ESDs that enable them: 1) ESDs should provide a reasonable level of autonomy to the system (state of charge (SOC) [1]); 2) ESDs should require a brief period of time to accumulate the necessary amount of energy that guarantees autonomy; and 3) ESDs should allow to be reused for a large number of operating cycles (i.e., the end user expects ESDs with extended life cycle).

The problem lies in the fact that brief charging periods and aggressive usage profiles generally affect the state of health (SOH) [2], and thus the remaining useful life (RUL) [3] of the ESD, in a negative way. This has motivated research not only in novel configurations and optimal charging profiles but also in the development of novel combinations of chemical elements that may secure rechargeable ESDs with a greater life cycle, e.g., lithium-ion (Li-ion) batteries [4].

Traditional approaches to battery health management have mostly focused on addressing the SOC issue with limited attention to SOH [1]. In many simpler systems, like the battery of a cell phone or a laptop computer, it is sufficient to approximate the RUL of the battery with a precision in a scale of months of operation since replacements are easy to obtain and affordable. In more complex systems (such as that of hybrid and electric vehicles) though, it is critical to determine when the ESD is approaching its end of life (EOL) with a precision of just a few cycles of operation. This task can only be accomplished through the implementation of accurate prognostic algorithms [3] to determine the number of remaining recharge cycles and the incorporation of real-time measurements of process and environmental variables (e.g., power consumption profile and temperature).

Online prognostic algorithms—and more specifically those based on sequential Monte Carlo (SMC) methods [a.k.a. particle filters (PFs)] [3]—are especially suitable to solve the aforementioned problem, given their capability to combine information available from system measurements and analytic/empirical models [3], [5]. Some ESDs (e.g., Li-ion and lead/acid batteries), however, suffer sudden regeneration (or self-recharge) phenomena [1], [5] that directly affect the precision and accuracy of that type of algorithms. This has only been briefly mentioned and studied in the current state of the art [5].

Manuscript received March 30, 2012; revised June 20, 2012; accepted July 23, 2012. Date of publication September 13, 2012; date of current version December 29, 2012. This work was supported by CONICYT under Project Fondo Nacional de Desarrollo Científico y Tecnológico 1110070. The Associate Editor coordinating the review process for this paper was Dr. Kurt Barbe.

B. E. Olivares and M. A. Cerda Muñoz are with the Department of Electrical Engineering, Universidad de Chile, Santiago 8370459, Chile.

M. E. Orchard and J. F. Silva are with the Department of Electrical Engineering, Universidad de Chile, Santiago 8370459, Chile, and also with the Advanced Mining Technology Center of the Universidad de Chile, Santiago 8370451, Chile (e-mail: morchard@ing.uchile.cl; josilva@ing.uchile.cl).

Color versions of one or more of the figures in this paper are available online at http://ieeexplore.ieee.org.

Digital Object Identifier 10.1109/TIM.2012.2215142

This paper presents a solution to the problem of simultaneous SOH and RUL estimation in ESDs, particularly addressing the detection of regeneration phenomena in Li-ion batteries through the implementation of particle-filtering-based detection and prognostic frameworks [3], [5]. This approach considers the use of state-space stochastic models for the characterization of battery degradation processes, mainly because of their ability to effectively combine empirical and phenomenological knowledge in the representation of nonlinear dynamic phenomena as well as their enabling capability for the implementation of Bayesian algorithms for the estimation of unobserved model parameters in the presence of non-Gaussian sources of uncertainty (allowing, for example, statistical characterization of self-recharge phenomena within the structure of the life-cycle model). Among the main contributions of this paper, the following can be mentioned: 1) It provides a framework capable of estimating the SOH while simultaneously detecting and isolating the effect of self-recharge phenomena on the initial conditions of predictive models (thus improving the performance of prognostic modules); 2) it presents guidelines to define the number of particles and realizations to use in a PF-based prognostic scheme to properly characterize the RUL probability density function (pdf) on the basis of analytical results for a simplified degradation model; and 3) it proposes novel *ad hoc* prognostic performance measures that incorporate the concept of "risk" within the analysis of prediction results.

This paper is organized as follows. Section II presents a theoretical background on the problem of SOH estimation in ESDs and failure prognosis based on PFs. Section III focuses on modeling aspects that are required to incorporate self-recharge phenomena in the prognostic framework. Section IV shows the implementation of the proposed approach for a hypothetical and simplified degradation system where the optimal solution (in the mean-square sense) can be found analytically with the purpose of comparing and analyzing the performance of the proposed approach in a controlled scenario. Section V shows the results achieved by the proposed SOH prognosis framework when used to estimate the RUL of Li-ion batteries that exhibit self-recharge phenomena in actual (accelerated) degradation tests. A comprehensive analysis of the obtained results, based on *ad hoc* performance measures, is presented in Section VI. Finally, Section VII states the main conclusions of this paper.

II. Theoretical Background

A. SOH Estimation in ESDs

One of the most important issues associated to the problem of ESD monitoring is to determine what kind of degradation processes is at work and how many more missions/operating cycles can be supported by the energy accumulator. These concepts are generally encapsulated in the terms SOH and state of life (SOL) [1]. While SOH is predominantly a diagnostics issue, SOL is primary a concern of prognostic algorithms (since it implies to predict the evolution of SOH in time) [1]. Thus, a good SOH prognostic algorithm should be able to predict the remaining capacity for future cycles of operation with adequate accuracy (i.e., a measure of the gap between the ground-truth failure time and the expectation of the RUL) and precision (i.e., a measure of the uncertainty associated to the prediction) [3]–[5].

Degradation processes in energy accumulators are complex and strongly influenced either by temperature or operating conditions during charge/discharge cycles [6]–[8]. Whereas the SOH of ESDs can be characterized using several condition indicators (such as the internal resistance/impedance or conductance, life cycle, capacity degradation rate, self-discharge rate, and power quality features associated to charge/discharge cycles [9], [10]), most of commercial solutions currently available are limited to voltage monitoring, Coulomb counters, and internal impedance measurements [1], [2], [11]. On the one hand, Coulomb counting (a method directed to measure the charge flow of accumulators) aims to estimate the capacity of a battery through the integration of electric current during each charge/discharge cycle. However, this approach would require absolute knowledge about the future usage profile to allow predicting the evolution of the SOH in an accurate manner; not to mention that all measurements must be calibrated with respect to a reference point, which hinders the application of this method to discharge profiles that include changes in operation points. Alternatively, measurements of the ESD internal impedance can be used to characterize changes in the internal resistance of the energy accumulator as a function of the SOH degradation; However, since this internal impedance depends directly on the temperature profile, it is difficult to provide a dependable estimate of the SOH (and, therefore, to predict its evolution in time) in the case of Li-ion batteries. A good example of this type of monitoring approach is the analysis of the electrochemical impedance spectroscopy (EIS), a noninvasive method used massively in laboratory testing to observe the capacity degradation of batteries [12], [13], which is difficult to implement in commercial applications because it implies additional instrumentation and a very specific testing setup [14], [15].

Previous research efforts in the area of battery SOH estimation have explored the use of electrochemical models for energy accumulators, either building equivalent circuits or studying the relationship between battery degradation and very specific features (SOC, depth of discharge, or accumulator age) [16], [17]. The analysis of degradation processes, however, also requires the incorporation of predictive models for the implementation of a framework capable of simultaneous SOH filtering (analysis of the current state) and prognosis (analysis of future behavior). These predictive models should allow rapid parameter adaptation to minimize the effect of measurement inaccuracies and erroneous initial conditions as well as to incorporate changes in environmental and operating conditions within long-term predictions [1], [5], [10]. In this sense, Saha *et al.* [1] present the implementation of regression models for SOH prognosis using relevance vector machines (RVMs) to generate a prediction curve that incorporates information from EIS measurements for an accumulator. RVMs present a clear advantage over other regression techniques, such as the support vector machine [16], [18], since RVM allows implementing a Bayesian framework and thus provides statistical information of the algorithm output, the RUL of the battery. Other

techniques use combinations of neural networks [8], fuzzy logic [19], regressions [2], or distributed active learning to perform regression in RUL prediction problems [20].

If Coulomb counting is used as a method to estimate the capacity of ESDs (with the purpose of providing an adequate initial condition in predictive models) and given that degradation processes in accumulators are nonlinear and subject to uncertainties, it is natural to implement suboptimal Bayesian estimation techniques such as the extended Kalman filter [21], [22]. This approach intends to approximate the error covariance matrix associated to the state estimate, using a linearized version of the dynamic system that represents the ESD degradation. The problem arises when trying to propagate this estimate on time in m-step-ahead predictions, and consequently, approximation errors are too significant to be neglected [3].

SMC methods (a.k.a. PF) have also proved to be useful when trying to represent uncertainty in the prognosis of degradation processes [3], [5]. In [23], for example, the concept of Bayesian estimation is applied to integrate diagnosis and prognosis of the health status of the accumulator. The concept utilizes RVM to identify the model, while the PF is used for model parameter adaptation, noise estimation, and characterization of the operating conditions of the life cycle of the accumulator in the form of pdfs. A similar approach is found in [24], where Bayesian Monte Carlo is used to update the parameters of an empirical model, thus representing the prediction of the degradation process through pdfs. The shortcomings of these approaches are related with the fact that pure empirical models cannot combine the information that is provided by the knowledge about the process phenomenology with real-time measured data, under assumptions of non-Gaussian sources of uncertainty and considering the existence of nonlinear phenomena. However, these objectives can be achieved if nonlinear state-space stochastic models are used instead.

The regeneration or self-recharge phenomena in Li-ion batteries has been briefly mentioned in the literature [1], [5]. Specifically in the case of lithium-ion batteries, this phenomenon has been represented as a self-charging in the logger where certain operating conditions facilitate a sudden (and temporary) increment in the available capacity of the ESD at the next cycle. This condition has been modeled as an exponential process in [1] and [5], and although the authors in [1] recognize the significance of the effect that this phenomena has on the accuracy and precision of prognostic algorithms based on Bayesian methods, only Orchard *et al.* [5] provide a solution based on risk-sensitive PFs that shows some degree of improvement. In this sense, particularly considering the significant contribution of PF algorithms to the implementation of prognosis frameworks, it is deemed necessary to present a summary of the main aspects associated to the formulation of particle-filtering-based predictive modules, which follows next.

B. Particle-Filtering-Based Prognosis Framework for Faulty Dynamic Nonlinear Systems

Consider a sequence of probability distributions $\{\pi_k(x_{0:k})\}_{k\geq 1}$, where it is assumed that $\pi_k(x_{0:k})$ can be evaluated pointwise up to a normalizing constant. SMC methods, also referred to as PFs, are a class of algorithms designed to approximately obtain samples from $\{\pi_k\}$ sequentially, i.e., to generate a collection of $N \gg 1$ weighted random samples $\{w_k^{(i)}, x_{0:k}^{(i)}\}_{i=1\ldots N}$, $w_k^{(i)} \geq 0, \forall k \geq 1$, satisfying [25], [26]

$$\sum_{i=1}^{N} w_k^{(i)} \varphi_k\left(x_{0:k}^{(i)}\right) \xrightarrow{N \to \infty} \int \varphi_k(x_{0:k}) \pi_k(x_{0:k}) dx_{0:k} \quad (1)$$

in probability, where φ_k is any π_k-integrable function.

In the particular case of the Bayesian filtering problem, the *target distribution* $\pi_k(x_{0:k}) = p(x_{0:k}|y_{1:k})$ is the posterior pdf of $X_{0:k}$, given a realization of noisy observations $Y_{1:k} = y_{1:k}$.

Let a set of N paths $\{x_{0:k-1}^{(i)}\}_{i=1\ldots N}$ be available at time $k-1$. Furthermore, let these paths distribute according to $q_{k-1}(x_{0:k-1})$, also referred to as the importance density function at time $k-1$. Then, the objective is to efficiently obtain a set of N new paths (particles) $\{\tilde{x}_{0:k}^{(i)}\}_{i=1\ldots N}$ distributed according to $\pi_k(\tilde{x}_{0:k})$ [25].

For this purpose, the current paths $x_{0:k-1}^{(i)}$ are extended by using the kernel $q_k(\tilde{x}_{0:k}|x_{0:k-1}) = \delta(\tilde{x}_{0:k-1} - x_{0:k-1}) \cdot q_k(\tilde{x}_k|x_{0:k-1})$, i.e., $\tilde{x}_{0:k} = (x_{0:k-1}, \tilde{x}_k)$. The importance sampling procedure generates consistent estimates for the expectations for any function, by approximating (2) with the empirical distribution [26]

$$\tilde{\pi}_k^N(x_{0:k}) = \sum_{i=1}^{N} w_{0:k}^{(i)} \delta\left(x_{0:k} - \tilde{x}_{0:k}^{(i)}\right) \quad (2)$$

where $w_{0:k}^{(i)} \propto w_{0:k}(\tilde{x}_{0:k}^{(i)})$ and $\sum_{i=1}^{N} w_{0:k}^{(i)} = 1$.

The most basic SMC implementation—the sequential-importance-sampling PF—computes the value of the particle weights $w_{0:k}^{(i)}$ by setting the importance density function equal to the *a priori* state transition pdf $p(\tilde{x}_k|x_{k-1})$, i.e., $q_k(\tilde{x}_{0:k}|x_{0:k-1}) = p(\tilde{x}_k|x_{k-1})$. In that manner, the weights for the newly generated particles are evaluated from the likelihood of new observations. The efficiency of the procedure improves as the variance of the importance weights is minimized. The choice of the importance density function is critical for the performance of the PF scheme, and hence, it should be considered in the filter design.

Prognosis, and thus the generation of long-term prediction, is a problem that goes beyond the scope of filtering applications since it involves future time horizons. Hence, if PF-based algorithms are to be used, it is necessary to propose a procedure with the capability to project the current particle population in time in the absence of new observations.

Any adaptive prognosis scheme requires the existence of at least one feature providing a measure of the severity of the fault condition under analysis (fault dimension). If many features are available, they can always be combined to generate a single signal. In this sense, it is always possible to describe the evolution in time of the fault dimension through the nonlinear state equation.

By using the aforementioned state equation to represent the evolution of the fault dimension in time, it is possible to generate m-step-ahead long-term predictions, using kernel

functions to reconstruct the estimate of the state pdf in future time instants, as it is shown in

$$\tilde{p}(x_{k+m}|\tilde{x}_{1:k+m-1}) \approx \sum_{i=1}^{N} w_{k+m-1}^{(i)} K\left(x_{k+m} - E\left[x_{k+m}^{(i)}|\tilde{x}_{k+m-1}^{(i)}\right]\right) \quad (3)$$

where $E(\cdot)$ represents the expectation of a random variable and $K(\cdot)$ is a kernel density function, which may correspond to the process noise pdf, a Gaussian kernel, or a rescaled version of the Epanechnikov kernel [3]. The resulting predicted state pdf contains critical information about the evolution of the fault dimension over time. One way to represent that information is through the computation of statistics (expectations, 95% confidence intervals), either the EOL [1] or the RUL of the faulty system [27].

The EOL pdf depends on both long-term predictions and empirical knowledge about the critical conditions for the system. This empirical knowledge is usually incorporated in the form of thresholds for main fault indicators. Therefore, the probability of failure at any future time instant $k = eol$ (namely, the EOL pdf) is given by

$$\Pr\{EOL = eol\} = \sum_{i=1}^{N} \Pr\left(Failure|X = \hat{x}_{eol}^{(i)}\right) \cdot w_{eol}^{(i)}. \quad (4)$$

The conditional probability of failure in (4) may be defined through the determination of hazard zones [3], either using historical data or knowledge from process operators. The simplest case is where the concept of "failure" implies the instant when the fault feature crosses a given threshold. In that case, the probability of failure, conditional to the state, is equal to one if the state is exactly on the manifold that defines the threshold value.

III. Modeling of Self-Recharge Phenomena in Battery Prognostic Modules

Several features are, directly or indirectly, associated to the SOH of ESDs, among which are the usage profile and the environmental conditions [28]. This research studies one of the most critical features that affect the SOH, the life cycle, which represents the number of times that a battery can be recharged before its capacity falls below acceptable limits, typically considered around the 80%–70% of the nominal capacity.

Life cycle models usually consider a specific term that aims to incorporate part of the phenomenology that is present in the ESD degradation process. In the case of batteries, this term is the Coulomb efficiency, η_c, which is a measure of how much usable energy is expected for the discharge cycle in progress in comparison with the capacity exhibited by the ESD during the previous discharge cycle [4]. Equations (5) and (6), inspired by the work presented in [1], show how this term can be included in a nonlinear dynamic model that can be used for SOH estimation purposes, hereafter denoted as "model #1":

State transition model

$$\begin{cases} x_1(k+1) = \eta_c x_1(k) + x_2(k)x_1(k) + \omega_1(k) \\ x_2(k+1) = x_2(k) + \omega_2(k) \end{cases} \quad (5)$$

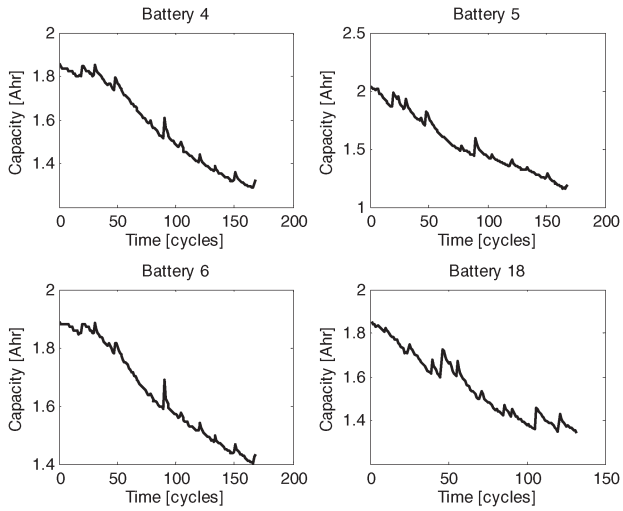

Fig. 1. Data set examples showing the results of accelerated degradation test in Li-ion batteries (NASA Ames Prognostics Center of Excellence).

Measurement equation

$$y(k) = x_1(k) + v(k) \quad (6)$$

where k is the cycle index; x_1 is a state representing the battery SOH; x_2 is a state associated with an unknown model parameter that is required to explain minor differences with respect to the expected behavior (which are specific to the monitored ESDs); $y(k)$ is the measured SOH; and ω_1, ω_2, and v are non-Gaussian noises.

Although "model #1" enables the implementation of Bayesian filtering techniques to monitor degradation processes in ESDs, it is inadequate when trying to detect and isolate the long-term effect of regeneration (self-recharge) phenomena in batteries. Self-recharge phenomena are characterized by sudden, momentary, and occasionally considerable regeneration of the battery capacity (see Fig. 1) that tends to fade in time faster than the typical SOH degradation time constant. These changes, related to physicochemical aspects and temperature/load conditions during charge and discharge cycles, are particularly important in the case of Li-Ion batteries because they often alter the trend of the SOH prediction curve, thus affecting the performance of prognostic modules based on Bayesian algorithms to estimate the initial conditions of their predictive models; see Fig. 1 showing the results of an accelerated degradation test performed on Li-ion batteries at the National Aeronautics and Space Administration (NASA) Ames Prognostic Center of Excellence [29].

Considering the previous point, a second state-space model is proposed in this work to solve the aforesaid issue and improve the quality of prognostic modules for the supervision of ESD degradation processes (see (7) and (8), hereafter denoted as "model #2"). Instead of using models based on the ESD physicochemical structure that may prove to be complex and offer little adaptation in real-time applications, "model #2" offers an empirical representation of regeneration phenomena that is used to quantify the long-term effect that the added ESD capacity has on the life cycle:

State transition model defined as in (7) and shown at the bottom of the next page.

Measurement equation

$$y(k) = x_1(k) + (\delta(1 - U(k)) + \delta(2 - U(k))) \cdot x_3(k) + v(k) \tag{8}$$

where x_3 is a state associated with the additional available SOH due to regeneration phenomena; U is a external input associated with the apparition of regeneration phenomena and is defined as in (9); $y(k)$ is the measured SOH; ω_{31} and ω_{32} are non-Gaussian noises used to represent uncertainty sources within the parameter estimation procedure; and $\delta(\cdot)$ is the delta of the Kronecker function.

The system external input U is defined as the output of an online PF-based detection module [3], [30] that performs a hypothesis test (1% false alarm rate) for the measurement $y(k)$, considering the *a priori* one-step-ahead prediction of the system output as the pdf that characterizes the null hypothesis (self-recharge phenomena either do not exist or are fading in time). This PF-based detection module basically determines a time-varying threshold for the hypothesis test that directly depends on the position of the particles associated to the empirical *a priori* state distribution. The threshold is then computed as the largest scalar $T(k)$ such that the sum of the weights $w_k^{(i)}$ of all particles satisfying the inequality $x_1^{(i)}(k) \geq T(k)$ is greater than the desired false alarm rate α (more details can be found in [3]). On the one hand, if the null hypothesis is accepted, then $U(k) = 0$. Alternatively, if the null hypothesis is rejected at cycle k (i.e., measurement $y(k)$ is larger than the detection threshold for the 99% statistical confidence of the one-step-ahead prediction pdf [3]), then $U(k) = 1$. Once $U(k)$ is set to one, it can only be reset to 0 after the hypothesis "$x_3 = 0$" is accepted. The latter implies that, when $U(k) = 1$, either a regeneration phenomenon has been detected or the latest that was detected is currently fading. In addition, if the hypothesis test for $y(k)$ rejects the null hypothesis and $U(k-1) = 1$, then $U(k) = 2$. This is done to indicate that at least two regeneration phenomena have occurred within a few cycles of operation

$$U(k) = \begin{cases} 0 & \text{if self-recharge does not exist} \\ 1 & \text{if either self-recharge is detected at cycle } k \\ & \text{or self-recharge phenomenon is fading} \\ 2 & \text{if additional self-recharge phenomena are} \\ & \text{detected before the latest one fades.} \end{cases} \tag{9}$$

The procedure to adequately determine the most appropriate noise kernels in "model #2" considered the isolation and statistical analysis of 68 self-recharge phenomena that occurred during Li-ion battery accelerated degradation tests at the NASA Ames Prognostic Center of Excellence (tests were performed at 23 °C, using a 2 A constant discharge current and assuming degradation when battery capacity falls below 75% of the nominal value of 2 Ah) [29]. The statistical analysis aimed at determining the most suitable distributions $\omega_{31}(k)$ and $\omega_{32}(k)$ that could be utilized to characterize uncertainty sources for the magnitude and typical damping ratio of regeneration phenomena, respectively, using the software STAT::FIT and considering the Kolmogorov–Smirnov goodness-of-fit test [31] (see Fig. 1). In this sense, it was found that the most appropriate distribution for noise kernel $\omega_{31}(k)$ (which characterizes the typical amount of SOH that is added in the event of successive regeneration phenomena) is log-normal. Analogously, for the case of the positive random variable $\omega_{32}(k)$ (which helps to characterize the typical damping ratio of self-recharge phenomena), the most appropriate distribution results to be uniform over the range [0.75, 0.85]. Distribution parameters both for $\omega_{31}(k)$ and $\omega_{32}(k)$ were also determined from this statistical study. Fig. 2 shows the performance of the resulting PF-based detector in the event of three regeneration phenomena, two of which are successive.

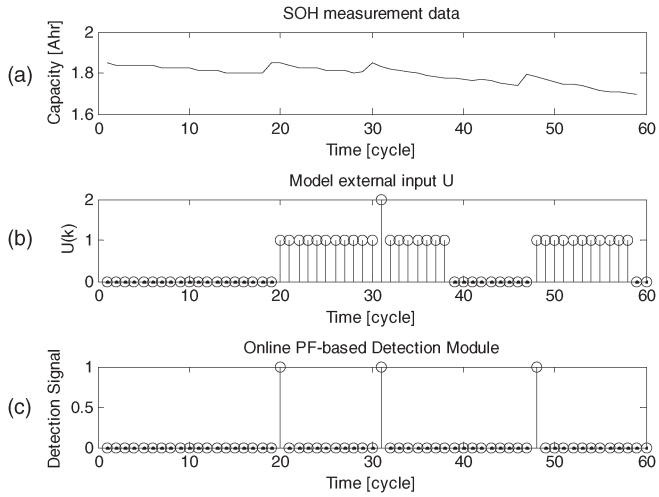

Fig. 2. PF-based detection framework for self-recharge phenomena for three regeneration events. (a) Actual SOH degradation data. (b) Model external input $U(k)$, generated according to (9). (c) Output of the PF-based detection module.

Equations (7)–(9) not only allow the implementation of suboptimal Bayesian estimation techniques within real-time prognostic modules but also allow a statistical characterization of self-recharge phenomena both in terms of frequency of occurrence and amplitude. Particle-filtering-based prognostic algorithms are especially suitable to accomplish the aforesaid task since they allow the inclusion of deterministic and probabilistic load profiles in predictive models [32]. However, it is first critical to determine how many realizations of the filter and how many particles are required to achieve a determined performance level for a specific prognostic application. In this sense,

$$\begin{cases} x_1(k+1) = \eta_c x_1(k) + x_2(k) x_1(k) + \omega_1(k) \\ x_2(k+1) = x_2(k) + \omega_2(k) \\ x_3(k+1) = \delta(U(k))\,\omega_{31}(k) + \delta(1 - U(k))\,(x_3(k)\omega_{32}(k)) \\ \qquad\qquad + \ldots \delta(2 - U(k))\,(x_3(k) + \omega_{31}(k)) \end{cases} \tag{7}$$

the following section of this paper focuses on a hypothetical and simplified degradation system where the optimal solution (in the mean-square sense) can be found analytically.

IV. PF-Based Prognosis for ESDs With Statistical Characterization of SOH Regeneration Phenomena

This section provides a comprehensive analysis of the main aspects that should be considered in the implementation of a particle-filtering-based framework for SOH prognosis in ESDs, with statistical characterization of self-recharge phenomena in batteries. In particular, the solution provided by the proposed PF-based approach is compared—in terms of accuracy of EOL expectation and just-in-time point ($JITP$ [33])—with the optimal (in the mean-square-error sense) *a priori* solution of the prediction problem for a hypothetical degradation process represented by a linear dynamic system.

A. Simplified Degradation Model and Analytical Solution for the SOH Prognosis in ESDs

The analytical solution for the problem of SOH degradation in ESDs may prove to be complex to obtain due to the fact that the process is nonlinear and non-Gaussian. In this regard, the utilization of a simplified scenario, where the degradation is described by a linear Gaussian dynamic system, offers the opportunity to compare the performances of suboptimal approaches, as well as the most appropriate values for design parameters. Regardless of what is stated earlier, the simplified version of the degradation process still includes part of the phenomenology of the process by incorporating the concept of Coulomb efficiency η_c, as seen in (10) and (11):

State transition model

$$\begin{cases} x_1(k+1) = \alpha_1 x_1(k) + \omega_1(k) \\ x_2(k+1) = \alpha_2 x_2(k) + \beta U(k) + \omega_2(k) \end{cases} \tag{10}$$

Measurement equation

$$y(k) = x_1(k) + x_2(k) + v(k) \tag{11}$$

where k is the cycle index; x_1 is a state representing the battery SOH; x_2 is a state associated with additional available SOH due to regeneration phenomena; α_1, α_2, and β are model parameters; U is an external input ($U(k) = 1$ if a regeneration phenomenon is detected at cycle k; else, $U(k) = 0$); $y(k)$ is the measured SOH; and ω_1 and ω_2 are independent zero-mean Gaussian noise terms with variances R_{ww1} and R_{ww2}, respectively. In this particular case, $\alpha_1 = \eta_c$.

The statistical characterization of self-recharge phenomena is implemented through a two-state first-order Markov chain [34] (being the null state associated to the absence of capacity regeneration, $U(k) = 0$) and transition probabilities estimated from the analysis of the 68 capacity regeneration events that were detected on actual accelerated degradation data (collected at the NASA Ames Prognostic Center of Excellence [29]). The resulting simplified model captures two key elements that can be identified in battery degradation processes: 1) Effectively, the long-term trend of the degradation curve can be coarsely approximated by a decreasing exponential function (see Fig. 1), and 2) indeed, the appearance of regeneration phenomena has a random component, being more frequent when operating the battery at high temperatures. There are, however, costs associated to the utilization of a simplified linearized model: 1) The structure assumes that the magnitude of regeneration effects is constant (β, a fixed model parameter) and independent of the number of previously detected events, and 2) the damping rates for both the long-term degradation term and self-recharge phenomena are fixed and temperature independent.

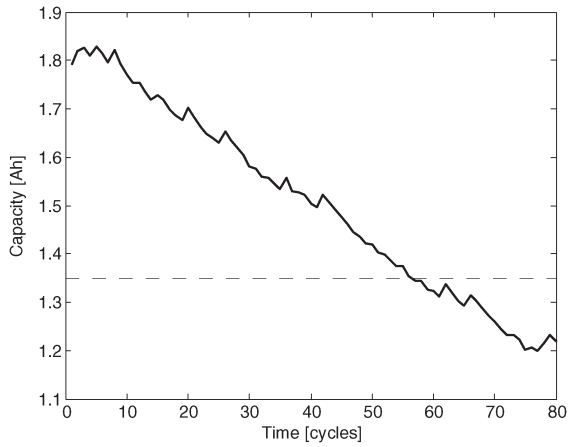

Fig. 3. Data generated by simplified model of SOH degradation in Li-ion batteries.

Fig. 3 shows a realization of the model defined by (10) and (11). These data will be used to compare the performance of the proposed PF-based SOH prognosis framework for ESDs versus the optimal solution, which can be obtained analytically using the *a priori* prediction equations of the Kalman filter. In this sense, it is important to mention that simulated data have considered a faster degradation constant (compared to the actual degradation test) to provide the means of comparing the performance of the aforementioned algorithms for a prediction window of 60–80 cycles of operation, which is considered reasonable for prognosis purposes [5].

Kalman filter equations formulate that the optimal one-step-ahead prediction for the state in a linear dynamic system is given by a Gaussian random variable with expectation given by (12) and covariance matrix defined by (13)

$$\hat{x}(k+1) = A\hat{x}(k) + Bu(k) \tag{12}$$

$$P(k+1) = AP(k)A^T + R_{ww} \tag{13}$$

where $\hat{x}(k)$ represents the state expectation; A and B are matrices that define the state equations of the linear system; $P(k)$ is the state covariance matrix at the kth discharge cycle; and R_{ww} is the process noise covariance matrix. In the particular case of model (10) and (11), it is possible to obtain closed-form expressions for the state predictions at the kth discharge cycle, for given initial conditions at the zeroth cycle of operation, by iterating (12) and (13). This information is sufficient to compute the EOL pdf for the simulated system.

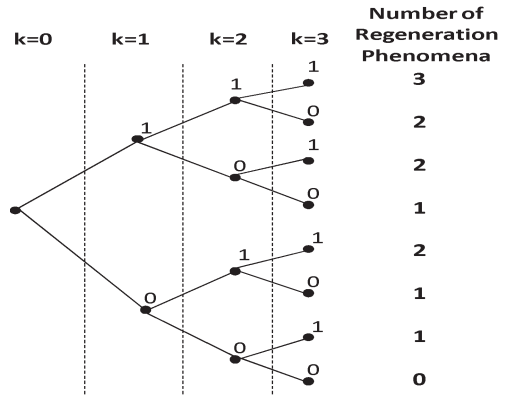

Fig. 4. Binary tree depicting the probability of self-recharging phenomena.

Particularly, for state x_1, it follows that

$$x_1(k) \sim N\left(\mu_{x_1}(k), \sigma^2_{x_1}(k)\right) \tag{14}$$

$$\mu_{x_1}(k) = \alpha_1 \mu_{x_1}(k-1) = \alpha_1^k \mu_{x_1}(0) \tag{15}$$

$$\begin{aligned}\sigma^2_{x_1}(k) &= \alpha_1^2 \sigma^2_{x_1}(k-1) + R_{ww1} \\ &= \alpha_1^{2k}\sigma^2_{x_1}(0) + R_{ww1}\sum_{i=0}^{k-1}\alpha_1^{2i}\end{aligned} \tag{16}$$

where the initial conditions of the state x_1 are assumed to be constant and defined by

$$\mu_{x_1}(0) = \mu_{x_1\,0}; \sigma^2_{x_1}(0) = \sigma^2_{x_1\,0}. \tag{17}$$

In the case of the second state of the simplified degradation system (x_2), the occurrence of future self-recharge phenomena must consider the stationary probability of the Markov chain that characterizes the transitions from the null state (absence of SOH regeneration) to the other state of the chain that represents the appearance of a regeneration phenomenon. Indeed, for each state transition in time, two possible scenarios may take place, and thus, the future evolution of state x_2 may be described using a binary decision tree. Fig. 4 shows this situation explained earlier, indicating possible paths that the state x_2 may follow when analyzing three-step-ahead predictions, conditional to the appearance of future self-recharge phenomena. In this case, the distribution for the predicted state x_2 results in the Gaussian mixture of the form

$$x_2(k) \sim \sum_{j=1}^{2^k} \omega_{j,k} N\left(\mu^{(j)}_{x_2}(k), \sigma^2_{x_2}(k)\right) \tag{18}$$

where k is the prediction time and the weights $\omega_{j,k}$ are computed recursively as follows:

$$\omega_{j,k} \triangleq \begin{cases} \omega_{j/2,k-1}\cdot\pi_1 & \text{if } j \text{ is even} \\ \omega_{(j+1)/2,k-1}\cdot\pi_0 & \text{if } j \text{ is odd} \end{cases}. \tag{19}$$

In (19), π_0 and π_1 represent the stationary probability for the Markov chain states associated to either the absence of SOH regeneration and the occurrence of the aforesaid phenomenon, respectively (their values were computed empirically from the accelerated degradation test in [29]). As a result, weights associated to even values of the j index in (18) intend to incorporate the probability of an additional regeneration phenomenon occurring at the prediction time of interest. The initial condition for the weights in the recursion is given by $\omega_{1,0} = 1$.

The corresponding expectations and state variances are given by

$$\mu^{(j)}_{x_2}(k) \triangleq \begin{cases} \mu^{(j)}_{x_2}(k-1)\cdot\alpha_2 + \beta & \text{if } j \text{ is even} \\ \mu^{(j+1)/2}_{x_2}(k-1)\cdot\alpha_2 & \text{if } j \text{ is odd} \end{cases} \tag{20}$$

$$\begin{aligned}\sigma^2_{x_2}(k) &= \alpha_2^2\sigma^2_{x_2}(k-1) + R_{ww2} \\ &= \alpha_2^{2k}\sigma^2_{x_2}(0) + R_{ww2}\sum_{i=0}^{k-1}\alpha_2^{2i}\end{aligned} \tag{21}$$

where the state initial condition distributes as a Gaussian pdf with expectation $\mu^{(1)}_{x_2}(0) = 0$ and variance $\sigma^2_{x_2}(0) = \sigma^2_{x_2\,0}$.

Given that SOH prognosis depends on the instant where the predicted value of the measured variable $y(k)$ reaches a determined threshold for the ESD capacity, it is also necessary to determine the analytic solution for the optimal *a priori* prediction of the system output $y(k)$. The latter can be obtained using

$$f_{Y(k)}\left(y(k)\right) = f_{X_1(k)}\left(x_1(k)\right) * f_{X_2(k)}\left(x_2(k)\right) \tag{22}$$

$$\begin{aligned}f_{Y(k)}\left(y(k)\right) &= N\left(\mu_{x1}(k), \sigma^2_{x_1}(k)\right) \\ &\quad * \sum_{j=1}^{2^k}\omega_{j,k}N\left(\mu^{(j)}_{x_2}(k), \sigma^2_{x_2}(k)\right).\end{aligned} \tag{23}$$

As a consequence, the output variable $y(k)$ also distributes as a Gaussian mixture characterized by

$$y(k) \sim \sum_{j=1}^{2^k}\omega_{j,k}N\left(\mu^{(j)}_{y}(k), \sigma^2_{y}(k)\right) \tag{24}$$

$$\mu^{(j)}_y(k) = \mu_{x_1}(k) + \mu^{(j)}_{x_2}(k) \tag{25}$$

$$\sigma^2_y(k) = \sigma^2_{x_1}(k) + \sigma^2_{x_2}(k). \tag{26}$$

At this point, it is important to notice that the first two moments of the Gaussian mixture (24) can be approximated respectively by [35]

$$\mu^{eq}_y(k) = \sum_{j=1}^{2^k}\omega_{j,k}\mu^{(j)}_y(k), \text{ and} \tag{27}$$

$$\begin{aligned}\sigma^{2\ eq}_y(k) &= \sum_{j=1}^{2^k}\omega_{j,k}\left(\sigma^2_y(k) + \left(\mu^{(j)}_y(k)\right)^2\right) \\ &\quad - \left(\mu^{eq}_y(k)\right)^2.\end{aligned} \tag{28}$$

This fact eases the computation of the first two moments of the failure time pdf (for this case, equivalent to the EOL). Also, if the failure SOH threshold (a.k.a. the hazard zone [3]) is fixed as a constant value at the 75% of the rated capacity, then the entire EOL pdf (for given specific initial conditions) may be computed by differentiating the cumulative density (29). Fig. 5 shows the resulting EOL pdf for given initial conditions at $k = 0$

$$\Pr\{EOL = eol\} = \int_{-\infty}^{SOH\ threshold} f_{Y(eol)}\left(y(eol)\right)d\left(y(eol)\right). \tag{29}$$

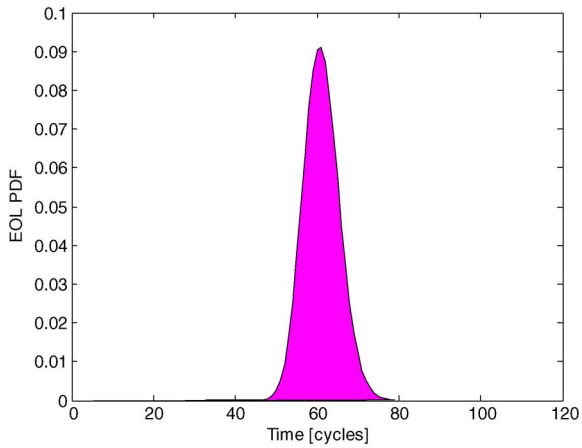

Fig. 5. EOL pdf (simplified degradation model).

Although the expected EOL, as in (30), is one the most common performance measures that are used to evaluate the accuracy of prognostic algorithms [5], it must be noted that a decision based on that value does not consider the fact that the probability of failing before the expected EOL cycle could be even close to 50% (obviously undesirable). In this regard, the JITP value (31) incorporates the concept of "risk," specifying the cycle of operation where the probability of failure reaches a specified threshold, given a probabilistic model for the degradation process

$$\hat{EOL} \triangleq E\{k|E\{y(k)\} = SOH\ threshold\} \quad (30)$$

$$JITP_{\alpha\%} = \arg\min_{k} \left(\Pr\{EOL \leq eol\} \geq \alpha\%\right). \quad (31)$$

Both measures will be used to compare the performance of the proposed PF-based approach for SOH prognostics with respect to the distribution that is computed from (29), as follows next.

B. PF-Based SOH Prognosis Framework in ESDs: Implementation Issues and Performance Analysis

The formulation of PF-based prognostic approaches has been widely covered in the literature [3], [5], [36]–[38]. However, there are specific issues associated to the implementation of these schemes that depend strongly on the number of states of the dynamic system and the type of nonlinearities exhibited by them. For this reason, it is important to determine the best algorithm parameters that should be used in prognostic applications oriented to SOH monitoring in ESDs. More specifically, focus is on the following: 1) the number of particles that need to be considered to represent the state pdf in each realization of the stochastic predictive model and 2) the number of realizations of the filtering algorithm that are required to ensure given standards in terms of accuracy of the predicted EOL pdf.

For this purpose, several experiments were conducted for a PF-based SOH prognostic algorithm using the simplified degradation model (10) and (11) in MATLAB R2009b simulation environment. Each experiment considered a different combination between the number of particles used in the implementation of the PF-based prognostic algorithm (minimum of 10 particles and maximum of 70 particles) and the number of realizations of the filter (1 to 70). The obtained results are compared to the analytic solution in terms of the $JITP_{\alpha\%}$ value and the EOL expectation. From one point of view, the $JITP_{\alpha\%}$ value is critical to define the number of particles that are needed to represent the uncertainty of the system since it provides information about the tail of the distribution. On the other hand, the accuracy on the EOL expectation (that is conditional to the occurrence of a SOH regeneration phenomenon) greatly depends on the number of realizations of the stochastic predictive model that are used to statistically characterize the degradation process.

TABLE I
EFFECT OF THE NUMBER OF PARTICLES ON $JITP_{\alpha\%}$ VALUE

$JITP_{\alpha\%}$	Analytic Solution	PF-based SOH Prognosis
$\alpha = 5$	53rd cycle	52nd cycle
$\alpha = 10$	54th cycle	53rd cycle

TABLE II
EFFECT OF THE NUMBER OF PF REALIZATIONS ON EOL EXPECTATION

$\hat{EOL}$	Analytic Solution	PF-based SOH Prognosis
40 realizations	62nd cycle	61st cycle

The obtained results showed that, for more than 50 particles in the PF-based SOH prognosis routine, the difference in terms of the $JITP$ value is almost negligible (one cycle). Table I shows the specific results obtained for two different $\alpha\%$, using 50 particles.

Analogously, after an exhaustive analysis of empirical results, it was determined that a PF-based SOH prognosis framework that uses 40 realizations of the particle-filtering algorithm, to characterize the initial condition of the predictive model, differs by only one cycle with respect to the analytic solution; see Table II.

These parameters have empirically proved to be adequate to implement a PF-based SOH prognostic module if a simplified degradation model is assumed, providing an important reference point for the implementation of the proposed prognostic scheme in the study of accelerated degradation test data, particularly when considering that nonlinearities in actual degradation processes make it impossible to replicate a similar study. This reference point not only helps to bound the effect of suboptimal estimation techniques in terms of accuracy and precision of the prognostic result but also helps to dimension the computational requirements associated to the implementation of the proposed prognostic solution.

V. VALIDATION OF A PF-BASED SOH PROGNOSIS FRAMEWORK IN EXPERIMENTAL DEGRADATION TEST

In this paper, the implementation of a PF-based SOH prognosis algorithm using (7)–(9) ("model #2") as state dynamic equations to describe the degradation process and a PF-based detection module [32] to detect and incorporate the effect of self-regeneration phenomena in long-term predictions is proposed. The proposed approach will be compared with the results available in the literature [1], [5], which are mainly based

on (5) and (6) ("model #1"). The most appropriate amount of particles (50 particles) and required realizations of the nonlinear filter (40 realizations) have been determined based on what was presented in Section IV. Validation data consider the results of the actual accelerated degradation test performed on Li-ion batteries at the NASA Ames Prognostic Center of Excellence [29]. Specifically, eight data sets were considered in this analysis for the determination of *a priori* knowledge, and one was considered for validation purposes. Each data set contained information for two different operating profiles, one for battery charge and the other for battery discharge, both at ambient temperature (23 °C). The battery nominal capacity is reported to be 2 Ah. Battery charging is performed using 1.5 A constant current (CC) until the battery voltage reaches 4.2 V; then, the rest of the charging procedure continues with constant voltage until the current drops below 20 mA. Battery discharge is performed using 2 A CC until the voltage drops below 2.5 V. The EOL criterion considers in this case the moment where the battery capacity drops below 75% of its nominal value. Although the figures presented in this section show validation results using one particular data set, similar results (in terms of accuracy and precision of the estimated EOL pdf) can be obtained independently of the data set that is used for that purpose.

Particle filtering can be used as in (2) and (3) to provide a sampled version of both filtered and predicted state pdfs. Furthermore, by finding the time instants where each particle trajectory reaches a given failure threshold, it is possible to compute a probabilistic characterization for the EOL of the system undergoing degradation, as shown in (4) and (29). Given that each particle trajectory strongly depends on the inner model that describes the degradation process, it is understandable that capacity regeneration phenomena could have a greater effect on prognostic frameworks based on "model #1" than on those based on the proposed "model #2." This is shown in Figs. 6 and 7, which respectively present the obtained results for PF-based SOH prognostic frameworks using "model #1" and "model #2" to describe degradation processes. Figs. 6(a) and 7(a) show the SOH measurement data (fine solid line) for an actual degradation test, the PF-based estimate (coarse solid line), and the PF-based prediction starting at the 60th discharge cycle (coarse dashed line). This prediction includes the expectation, as well as the lower and upper bounds of the 95% confidence interval for the predicted SOH, as a function of time. Figs. 6(b) and 7(b) show the computed EOL pdf, as well as 95% confidence intervals (dashed vertical lines) and the expectation of the EOL pdf (dark vertical line).

It is worth noting that Fig. 6(a) shows the effect of self-recharge phenomena (20th, 31th, and 48th cycles of operation) both on the filtering and the prognostic phases of the algorithm. In fact, it is extremely difficult to incorporate these events within the state estimates, greatly affecting their accuracy and also the initial condition for the prediction of SOH degradation. As a consequence, the EOL pdf [see Fig. 6(b)] evidences greater dispersion and variance than in the case of an approach based on "model #2" and, therefore, larger confidence intervals for the EOL of the ESD.

On the other hand, Fig. 7(a) shows the results of the prognosis scheme based on "model #2" and the PF-based diagnosis

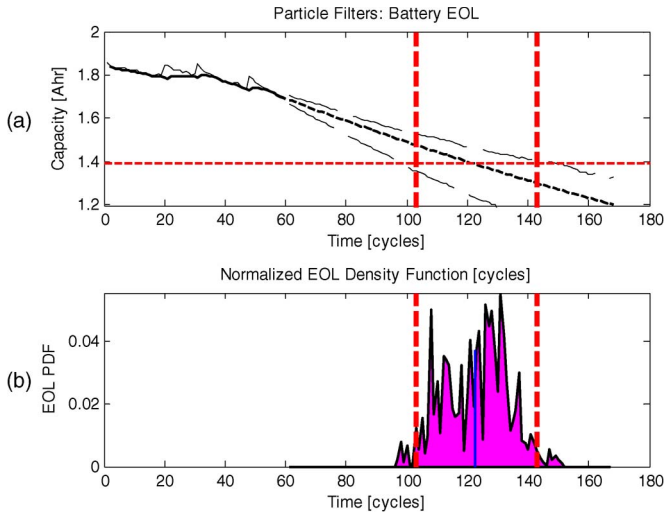

Fig. 6. EOL prediction based on model #1 [see (5) and (6)]. (Fine solid line) Measurement data. (Coarse solid line) PF-based estimate. (Coarse dashed line) PF-based prediction.

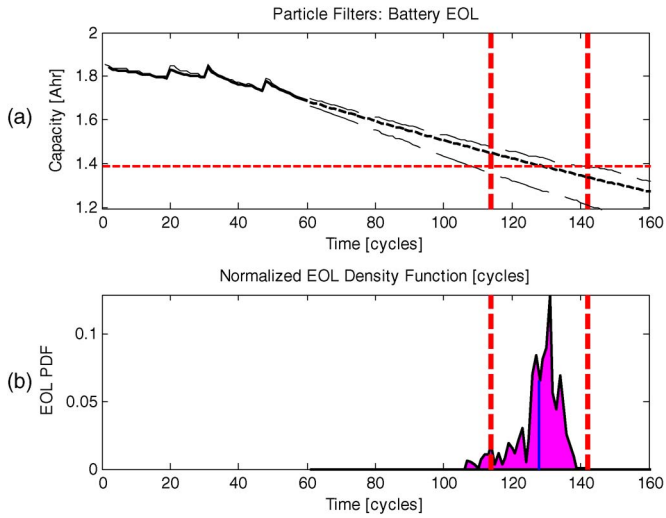

Fig. 7. EOL prediction based on model #2, which explicitly incorporates a detection module for regeneration phenomena. (Fine solid line) Measurement data. (Coarse solid line) PF-based estimate. (Coarse dashed line) PF-based prediction.

module for the detection of regeneration phenomena [that is used to determine the value of the external input signal $U(k)$ in (7)–(9)]. It is important to note that the detection module does not suffer from false positives (original design proposed 1% false alarm rate). Additionally, by observing the computed EOL pdf in Fig. 7(b), it can be noted that the prediction variance in the EOL pdf is smaller than in the case of the classic approach shown in Fig. 6(b). Furthermore, the accuracy of the prediction result improves when using "model #2."

From an implementation standpoint, it is important to mention that the algorithm complexity allows the computation of an EOL pdf estimate in approximately 2.84 s, using MATLAB R2009b environment and Advanced Micro Devices Athlon II P320 Dual-Core Processor 2.10 GHz (installed memory (RAM): 4 GB). According to this information, this algorithm could be easily embedded as part of a more integral solution for battery management systems (BMSs), providing more accurate and precise estimates of the ESD RUL. In this sense, it must be

noted that the avoidance of battery RUL overestimation has a direct impact in logistics (since it is possible to know exactly when to change the battery), recycling-oriented businesses, and battery certification procedures for used electrical vehicles.

Although visual evidence could be a good indicator of the improvements that can be obtained by using the proposed model within the PF-based SOH prognosis module, it is necessary to define appropriate performance measures to quantify and evaluate that improvement in a more rigorous manner. The following section focuses on this specific topic, which is of paramount importance for a correct interpretation of the obtained results.

VI. Prognostic Performance Measures and Evaluation of the Proposed SOH Degradation Monitoring Approach

It is widely accepted within the prognostic and health management community that the quality of forecasts and prognostic approaches is directly related to the accuracy and precision of the EOL/RUL estimates [32], [36]–[38]. Although some authors have proposed prognostic performance measures in the past [5], [39], not necessarily those indicators represent the most important aspects to be considered in a specific application such as SOH prognosis for ESDs. Typical accuracy and precision metrics assume that the risk associated to accuracy problems is equivalent for the case where the EOL is either overestimated or underestimated. This is clearly not true in the case of failure prognosis problems. In addition, metrics such as RMS error assume that the system is time invariant (which is not necessarily true) and cannot capture the fact that the risk associated to accuracy problems increases as the RUL diminishes. Although it is possible to consider a weighted version of those metrics, it is not straightforward to define the weights as a function of the risk function. This section aims at filling this gap, proposing *ad hoc* performance measures that could help to analyze the results obtained for the case of accelerated degradation tests and identifying the main improvements associated to the use of "model #2" within the implementation of a PF-based prognostic framework for SOH degradation monitoring.

A. Prognostic Accuracy Measure

Accuracy is a bias measure of the prognostic algorithm, which basically can be computed as the difference between the expected EOL of the system and its ground-truth value

$$Accuracy = \varphi\left(EOL - E\left\{EOL|y_{1:k_{pred}}\right\}\right)_{\forall k_{pred}\in[1,EOL]} \tag{32}$$

where EOL is the ground-truth EOL, k_{pred} is the cycle where the prognostic algorithm is executed, $E\{EOL|y_{1:k_{pred}}\}$ is the conditional expectation given the observed data, and φ is a logistic function that aims to scale the results in the range $[-1, 1]$. For this measure, the better the accuracy is, the smaller the measure's absolute value is ($\varphi = 0$ indicates perfect accuracy). It is important to note that this measure only allows quantifying the average quality of the prediction and is not for a particular experiment (that could easily be part of the tail of the probability distribution).

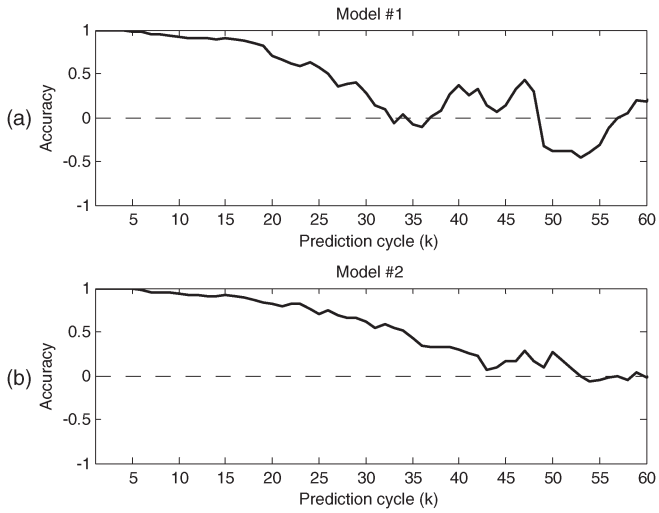

Fig. 8. Evaluation of PF-based SOH prognostic module using the proposed accuracy performance measure and (a) model #1 or (b) model #2.

Fig. 8 shows the evaluation of the PF-based SOH prognostic algorithm using "model #1" [see Fig. 8(a)] and "model #2" [see Fig. 8(b)], considering the long-term predictions that were generated (emulating real-time operation) at each discharge cycle k_{pred}. Given that the prediction algorithm is based on Bayesian estimators, it would be expected that the accuracy should improve as the amount of information increases; however, it can be observed that there are instants where the proposed accuracy measure shows overestimation of the EOL (accuracy measure takes a negative value).

The aforesaid behavior is absolutely undesirable in any prognostic module since it implies that the ESD could fail before it was prognosticated. To this effect, a PF-based prognostic algorithm based on the proposed "model #2" exhibits better performance [see Fig. 8(b)] than its counterpart based on model #1, which tends to overestimate the RUL of the system during discharge cycles 49–57 [see Fig. 7(a)].

B. DSTD

Another important aspect to be considered in the evaluation of performance measures is the volatility of generated predictions, which could be measured by computing the standard deviation of the expected EOL over a sliding window

$$DSTD = \varphi\left(\sqrt{Var\left(E\{EOL|y_{1:j}\}\right)_{j=k_{pred}-\Delta:k_{pred}}}\right)_{\forall k_{pred}\in[1,EOL]} \tag{33}$$

where k_{pred} is the cycle where the prognostic algorithm is executed, Δ is the number of samples considered in the sliding window, and φ is the logistic function that aims to scale the results in the range [0,1]. For this measure, the better the dynamic standard deviation (DSTD), the closer to zero is the measure ($DSTD = 0$ indicates perfect null volatility and the fact that new measurements do not alter the output of the prognostic algorithm). Fig. 9 shows the evaluation of the PF-based

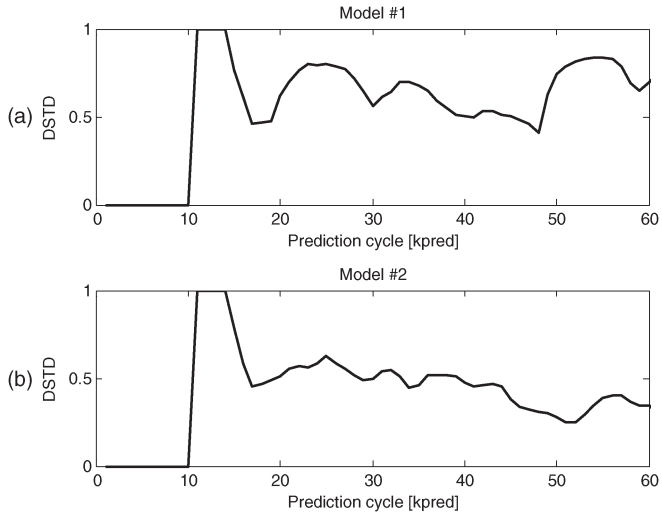

Fig. 9. Evaluation of PF-based SOH prognostic module using the proposed DSTD performance measure and (a) model #1 or (b) model #2.

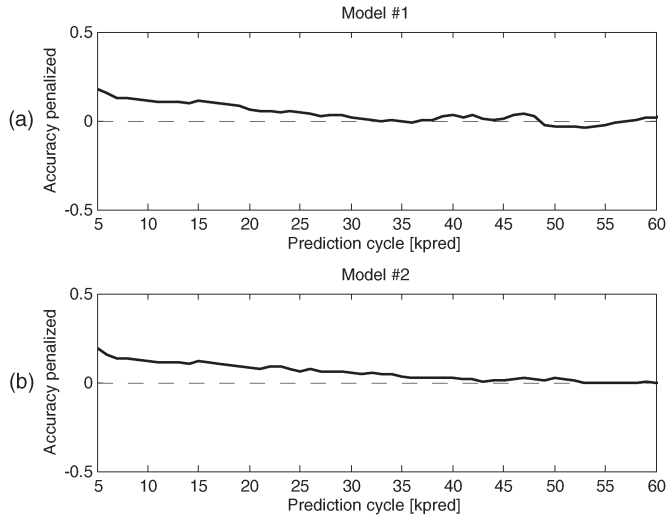

Fig. 10. Evaluation of PF-based SOH prognostic module using the proposed penalized accuracy performance measure and (a) model #1 or (b) model #2.

SOH prognostic algorithm using "model #1" [see Fig. 9(a)] and "model #2" [see Fig. 9(b)], considering the long-term predictions that were generated (emulating real-time operation) at each discharge cycle k.

Fig. 9(a) shows that self-recharge phenomena affect the volatility of long-term predictions based on "model #1" in a greater manner than in the case of "model #2" [see Fig. 9(b)]. In fact, the DSTD index is always greater in the former case than in the latter after the capacity regeneration phenomena (20th, 31th, and 48th cycles of operation). This is mainly caused by the better adaptation properties offered by "model #2," which allow improved estimation results and, therefore, better initial conditions for long-term predictions. This element is critical in terms of the assessment of prognostic algorithms since it is directly related to the precision of the forecast and the capability to absorb external perturbations.

C. Prognostic Accuracy Measure (Penalized)

This performance measure incorporates the fact that accuracy problems should be penalized if the system is close to the failure time (as any mistake could be costly)

$$Accuracy\_penalized = \varphi\left(\frac{EOL - E\left\{EOL|y_{1:k_{pred}}\right\}}{E\left\{RUL|y_{1:k_{pred}}\right\}}\right)_{\forall k_{pred}\in[1,EOL]} \quad (34)$$

where

$$E\left\{RUL|y_{1:k_{pred}}\right\} = E\left\{EOL|y_{1:k_{pred}}\right\} - k_{pred}. \quad (35)$$

Fig. 10 shows the effects of the penalty factor on the accuracy measure. The analysis of this figure provides information that is consistent with the result shown in Fig. 8.

D. Critical-α Performance Measure

Decision-making support systems cannot depend solely on information about the expectation of random variables since the tail of pdfs contains critical information about the risk that is associated to process operation. Ergo, a novel performance measure based on the concept of the JITP moment is hereby presented: the critical-α index.

The critical-α index is a measure of risk aversion (a significant factor to be considered when using implementations that overestimate the RUL of a system) and is defined as the maximum $\alpha \in [0, 100]$ that guarantees that the $\text{JITP}_{\alpha\%}(k_{pred})$ value is smaller than the ground-truth value of the ESD EOL time instant, for all $k_{pred} \in [1, \text{EOL}]$

$$\alpha_{crit} = \arg\max_{\alpha}\left\{JITP_{\alpha\%}(k_{pred}) \leq EOL\right\}_{\forall k_{pred}\in[1,EOL]}. \quad (36)$$

Decision-making support systems that consider prognostic algorithms with larger critical-α values in their design are capable of implementing more aggressive strategies. This is based on the fact that these prognostic routines are conservative, and then, it is possible to accept the risk of accumulating larger failure probability mass before recommending a corrective action. However, a large critical-α value is also an indicator that the variance of the predicted EOL pdf is large (i.e., less precise estimates of the EOL). For this reason, a good design should try to lessen this problem by selecting prognostic algorithms that allow not only to use large critical-α values but also to minimize—over time—the difference between the ground-truth EOL and the JITP values computed for the corresponding $\alpha_{crit}\%$. This difference is computed using the performance measure

$$Error\_\alpha_{crit} = \sum_{k_{pred}=1}^{EOL}\left(EOL - JITP_{\alpha_{crit\%}}(k_{pred})\right). \quad (37)$$

In this particular case of study, the implementation of the proposed SOH prognosis framework using "model #1" allows $\alpha_{crit} = 7.8$, compared to $\alpha_{crit} = 35.92$ that is obtained if the proposed "model #2" is used instead. In principle, this shows that the proposed model would allow the implementation of more aggressive decision-making support systems. Furthermore, the evaluation of the measure $Error\_\alpha_{crit}$ shows that the latter model also offers (for a given critical-α value) a more steady solution and less dispersion in the EOL pdf, making it

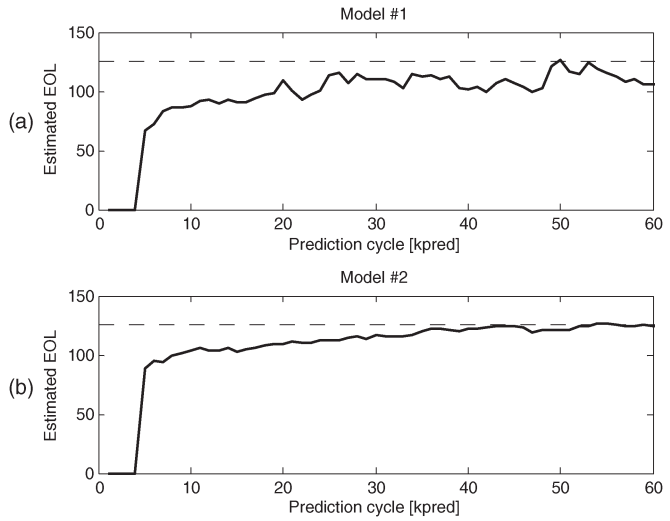

Fig. 11. PF-based SOH prognostic module performance. EOL estimate using JITP(k_{pred}), the critical-α value, and (a) model #1 or (b) model #2.

more suitable for the implementation of real-time decision systems; see Fig. 11, which compares the performance of the PF-based SOH prognosis module using model #1 [see Fig. 11(a)] and that using the proposed model #2 [see Fig. 11(b)] in terms of the difference between the ground-truth EOL (126th cycle, in this case) and the corresponding $JITP_{\alpha_{crit\%}}$ computed over time. In this sense, the proposed approach [see Fig. 11(b)] minimizes $Error\_{\alpha_{crit}}$, thus being selected as the best method among the two.

VII. Conclusion

This work has presented, evaluated, and validated a novel degradation model that enables the implementation of particle-filtering-based prognostic frameworks for SOH estimation and RUL prognosis in ESDs, and more specifically on Li-ion batteries. This model includes a statistical characterization of the self-recharge phenomena and an online PF-based detection module that performs a hypothesis test (1% false alarm rate) for SOH measurements to detect regeneration events in the battery life cycle, thus improving the initial condition that the scheme uses to generate long-term predictions.

The effectiveness of the proposed prognostic approach has been tested using a simplified degradation scenario where the optimal analytical solution of the prediction problem (in the mean-square sense) can be computed. As a result, optimal parameters for the implementation of the proposed approach were found, maximizing the accuracy of long-term predictions and the capability to represent the tail of the EOL pdf—the latter being represented by the JITP value of the aforementioned distribution. Additionally, the proposed PF-based framework has been validated using experimental data from accelerated degradation tests and a set of *ad hoc* performance measures to quantify the precision and accuracy of the estimates. Results show that the capability of detecting regeneration phenomena that is provided by the proposed model is a key element within the prognostic approach since it allows to improve the accuracy of the long-term prediction and to minimize the effect of perturbations in the variance of the predicted EOL pdf (thus helping to generate more reliable life cycle prognostics). A novel performance measure—the critical-α index—also indicates that the proposed approach is more appropriate to manage the risk that is associated to EOL predictions (a critical element in the design of decision-making support systems), when compared to other implementations available in the literature.

Regarding the impact of the proposed algorithm on BMSs, it must be noted that BMS performance increases as the quality of the information grows (since BMS needs to take decisions based on that information). In this sense, from the analysis of Figs. 8, 9, and 11, it is possible to infer that the proposed algorithm improves significantly the accuracy and precision of EOL and RUL estimates. Avoiding overestimation of the battery RUL will have a direct positive impact in logistics (it is possible to know exactly when to change the battery), recycling-oriented businesses, and battery certification procedures for used electrical vehicles. Future work will consider more specific phenomenology aspects within the modeling of battery degradation processes, such as the effect of temperature and outline usage in the physicochemical structure of ESDs.

Acknowledgment

The authors would like to thank the anonymous reviewers and Dr. C. Estevez for their valuable feedback.

References

[1] B. Saha, K. Goebel, S. Poll, and J. Christophersen, "Prognostics methods for battery health monitoring using a Bayesian framework," *IEEE Trans. Instrum. Meas.*, vol. 58, no. 2, pp. 291–296, Feb. 2009.

[2] B. Pattipati, K. Pattipati, J. P. Christopherson, S. M. Namburu, D. V. Prokhorov, and L. Qiao, "Automotive battery management systems," in *Proc. IEEE AUTOTESTCON*, Sep. 8–11, 2008, pp. 581–586.

[3] M. Orchard and G. Vachtsevanos, "A particle filtering approach for on-line fault diagnosis and failure prognosis," *Trans. Inst. Meas. Control*, vol. 31, no. 3/4, pp. 221–246, Jun. 2009.

[4] R. A. Huggins, *Advanced Batteries: Materials Science Aspects*. New York: Springer-Verlag, 2008.

[5] M. Orchard, L. Tang, B. Saha, K. Goebel, and G. Vachtsevanos, "Risk-sensitive particle-filtering-based prognosis framework for estimation of remaining useful life in energy storage devices," *Stud. Inf. Control*, vol. 19, no. 3, pp. 209–218, Sep. 2010.

[6] D. Danilov and P. H. L. Notten, "Adaptive battery management systems for the new generation of electrical vehicles," in *Proc. IEEE VPPC*, Sep. 7–10, 2009, pp. 317–320.

[7] M. Ichimura, M. Shimomura, K. Takeno, R. Shirota, and J. Yamaki, "Synergistic effect of charge/discharge cycle and storage in degradation of lithium-ion batteries for mobile phones," in *Proc. 27th INTELEC*, Sep. 2005, pp. 245–250.

[8] K. Qian, C. Zhou, Y. Yuan, and M. Allan, "Temperature effect on electric vehicle battery cycle life in vehicle-to-grid applications," in *Proc. CICED*, Sep. 13–16, 2010, pp. 1–6.

[9] F. Rufus, S. Lee, and A. Thakker, "Health monitoring algorithms for space application batteries," in *Proc. Int. Conf. PHM*, Oct. 6–9, 2008, pp. 1–8.

[10] P. E. Pascoe and A. H. Anbuky, "Standby VRLA battery reserve life estimation," in *Proc. 26th Annu. INTELEC*, Sep. 19–23, 2004, pp. 516–523.

[11] Y. Xing, Q. Miao, K.-L. Tsui, and M. Pecht, "Prognostics and health monitoring for lithium-ion battery," in *Proc. IEEE Int. Conf. ISI*, Jul. 10–12, 2011, pp. 242–247.

[12] F. Huet, "A review of impedance measurements for determination of state-of-charge or state-of-health of secondary batteries," *J. Power Sources*, vol. 70, no. 1, pp. 59–69, Jan. 1998.

[13] S. Rodrigues, N. Munichandraiah, and A. K. Shukla, "A review of state-of-charge indication of batteries by means of AC impedance measurements," *J. Power Sources*, vol. 87, no. 1/2, pp. 12–20, Apr. 2000.

[14] V. Pop, H. J. Bergveld, P. H. L. Notten, and P. P. L. Regtien, "State-of-the-art of battery state-of-charge determination," *Meas. Sci. Technol.*, vol. 16, no. 12, pp. R93–R110, Dec. 2005.

[15] S. Piller, M. Perrin, and A. Jossen, "Methods for state-of-charge determination and their applications," *J. Power Sources*, vol. 96, no. 1, pp. 113–120, Jun. 2001.
[16] B. Pattipati, C. Sankavaram, and K. Pattipati, "System identification and estimation framework for pivotal automotive battery management system characteristics," *IEEE Trans. Syst., Man, Cybern. C, Appl. Rev*, vol. 41, no. 6, pp. 869–884, Nov. 2011.
[17] S. Santhanagopalan, Q. Zhang, K. Kumaresan, and R. E. White, "Parameter estimation and life modeling of lithium-ion cells," *J. Electrochem. Soc.*, vol. 155, no. 4, pp. A345–A353, 2008.
[18] L. Chu, F. Zhou, and J. Guo, "Investigation of cycle life of Li-ion power battery pack based on LV-SVM," in *Proc. Int. Conf. MEC*, Aug. 19–22, 2011, pp. 1602–1605.
[19] A. J. Salkind, C. Fennie, P. Singh, T. Atwater, and D. E. Reisner, "Determination of state-of-charge and state-of-health of batteries by fuzzy logic methodology," *J. Power Sources*, vol. 80, no. 1/2, pp. 293–300, Jul. 1999.
[20] H. Chen and X. R. Li, "Distributed active learning with application to battery health management," in *Proc. 14th Int. Conf. FUSION*, Jul. 5–8, 2011, pp. 1–7.
[21] B. S. Bhangu, P. Bentley, D. A. Stone, and C. M. Bingham, "State-of-charge and state-of-health prediction of lead-acid batteries for hybrid electric vehicles using non-linear observers," in *Proc. Euro. Conf. Power Electron. Appl.*, pp. 1–10.
[22] D. Haifeng, W. Xuezhe, and S. Zechang, "A new SOH prediction concept for the power lithium-ion battery used on HEVs," in *Proc. IEEE VPPC*, Sep. 7–10, 2009, pp. 1649–1653.
[23] B. Saha and K. Goebel, "Uncertainty management for diagnostics and prognostics of batteries using Bayesian techniques," in *Proc. IEEE Aerosp. Conf.*, Mar. 1–8, 2008, pp. 1–8.
[24] W. He, N. Williard, M. Osterman, and M. Pecht, "Remaining useful performance analysis of batteries," in *Proc. IEEE Conf. PHM*, Jun. 20–23, 2011, pp. 1–6.
[25] C. Andrieu, A. Doucet, and E. Punskaya, "Sequential Monte Carlo methods for optimal filtering," in *Sequential Monte Carlo Methods in Practice*, A. Doucet, N. de Freitas, and N. Gordon, Eds. New York: Springer-Verlag, 2001.
[26] A. Doucet, N. de Freitas, and N. Gordon, "An introduction to sequential Monte Carlo methods," in *Sequential Monte Carlo Methods in Practice*, A. Doucet, N. de Freitas, and N. Gordon, Eds. New York: Springer-Verlag, 2001.
[27] L. Tang, M. E. Orchard, K. Goebel, and G. Vachtsevanos, "Novel metrics and methodologies for the verification and validation of prognostic algorithms," in *Proc. IEEE Aerosp. Conf.*, Mar. 5–12, 2011, pp. 1–8.
[28] R. Hartmann, "An Aging Model for Lithium-Ion Cells," Ph.D. dissertation, Univ. Akron, Akron, OH, 2008.
[29] NASA Ames, B. Saha and K. Goebel, "Battery data set," NASA Ames Prognostics Data Repository, Moffett Field, CA2007. [Online]. Available: http://ti.arc.nasa.gov/tech/dash/pcoe/prognostic-data-repository/
[30] B. Zhang, C. Sconyers, C. Byington, R. Patrick, M. Orchard, and G. Vachtsevanos, "A probabilistic fault detection approach: Application to bearing fault detection," *IEEE Trans. Ind. Electron.*, vol. 58, no. 5, pp. 2011–2018, May 2011.
[31] S. Guatelli, B. Mascialino, A. Pfeiffer, M. G. Pia, A. Ribon, and P. Viarengo,, "Application of statistical methods for the comparison of data distributions," in *Proc. IEEE Nucl. Sci. Symp. Conf. Rec.*, Oct. 16–22, 2004, vol. 4, pp. 2086–2090.
[32] D. Edwards, M. Orchard, L. Tang, K. Goebel, and G. Vachtsevanos, "Impact of input uncertainty on failure prognostic algorithms: Extending the remaining useful life of nonlinear systems," in *Proc. Annu. Conf. Prognostics Health Manag. Soc.*, Portland, OR, Oct. 10–14, 2010.
[33] S. J. Engel, B. J. Gilmartin, K. Bongort, and A. Hess, "Prognostics, the real issues involved with predicting life remaining," in *Proc. IEEE Aerosp. Conf.*, 2000, vol. 6, pp. 457–469.
[34] L. R. Rabiner, "A tutorial on hidden Markov models and selected applications in speech recognition," *Proc. IEEE*, vol. 77, no. 2, pp. 257–286, Feb. 1989.
[35] L. Trailovic and L. Y. Pao, "Variance estimation and ranking of Gaussian mixture distributions in target tracking applications," in *Proc. 41st IEEE Conf. Decision Control*, Dec. 10–13, 2002, vol. 2, pp. 2195–2201.
[36] M. Orchard, F. Tobar, and G. Vachtsevanos, "Outer feedback correction loops in particle filtering-based prognostic algorithms: Statistical performance comparison," *Stud. Inf. Control*, vol. 18, no. 4, pp. 295–304, Dec. 2009.
[37] B. Zhang, T. Khawaja, R. Patrick, G. Vachtsevanos, M. Orchard, and A. Saxena, "Application of blind deconvolution denoising in failure prognosis," *IEEE Trans. Instrum. Meas.*, vol. 58, no. 2, pp. 303–310, Feb. 2009.
[38] C. Chen, G. Vachtsevanos, and M. Orchard, "Machine condition prediction based on adaptive neuro-fuzzy and high-order particle filtering," *IEEE Trans. Ind. Electron.*, vol. 58, no. 9, pp. 4353–4364, Sep. 2011.
[39] A. Saxena, J. Celaya, B. Saha, S. Saha, and K. Goebel, "Evaluating prognostics performance for algorithms incorporating uncertainty estimates," in *Proc. IEEE Aerosp. Conf.*, Mar. 6–13, 2010, pp. 1–11.

Benjamín E. Olivares was born in Santiago, Chile, in 1987. He received the B.S. degree in electrical engineering from Universidad de Chile, Santiago, in 2011, where he is currently working toward the M.Sc. degree in the Department of Electrical Engineering.

He is a Research Engineer at the "Lithium Innovation Center," Santiago. His research interests include prognostics and health management for energy storage devices based on optimal and suboptimal Bayesian algorithms.

Matías A. Cerda Muñoz was born in Santiago, Chile, in 1987. He received the B.Sc. degree in electrical engineering from Universidad de Chile, Santiago, in 2011, where he is currently working toward the M.S. degree in the Department of Electrical Engineering.

He is a Research Engineer at the "Lithium Innovation Center," Santiago. His research interests include prognostics and health management for energy storage devices based on optimal and suboptimal Bayesian algorithms.

Marcos E. Orchard (M'06) received the B.S. degree and the Civil Industrial Engineering degree with Electrical Major from the Catholic University of Chile, Santiago, Chile, in 1999 and 2001, respectively, and the Ph.D. and M.S. degrees from the Georgia Institute of Technology, Atlanta, in 2005 and 2007, respectively.

He is currently an Assistant Professor with the Department of Electrical Engineering, Universidad de Chile, Santiago, and was part of the Intelligent Control Systems Laboratory, Georgia Institute of Technology. His current research interest is the design, implementation, and testing of real-time frameworks for fault diagnosis and failure prognosis, with applications to battery management systems, mining industry, and finance. His fields of expertise include statistical process monitoring, parametric/nonparametric modeling, and system identification. His research work at the Georgia Institute of Technology was the foundation of novel real-time fault diagnosis and failure prognosis approaches based on particle-filtering algorithms. Dr. Orchard has published more than 50 papers in his areas of expertise.

Jorge F. Silva (S'06–M'09) received the M.S. and Ph.D. degrees in electrical engineering from the University of Southern California (USC), Los Angeles, in 2005 and 2008, respectively.

He is currently an Assistant Professor with the Department of Electrical Engineering, University of Chile, Santiago, Chile. His research interests include nonparametric learning, sparse signal representations, statistical learning, universal source coding, sequential decision and estimation, distributive learning, and sensor networks.

Dr. Silva is IEEE member of the Signal Processing and Information Theory Societies, and he has participated as a reviewer in various IEEE journals on Signal Processing. He was the recipient of the Outstanding Thesis Award 2009 for Theoretical Research of the Viterbi School of Engineering, the Viterbi Doctoral Fellowship 2007–2008, and the Simon Ramo Scholarship 2007–2008 at USC.